

Review

Synergistically Enhancing the Therapeutic Effect on Cancer, via Asymmetric Bioinspired Materials

Yasamin Ghahramani ¹, Marzieh Mokhberi ², Seyyed Mojtaba Mousavi ^{3,*}, Seyyed Alireza Hashemi ⁴, Fatemeh Fallahi Nezhad ⁵, Wei-Hung Chiang ³, Ahmad Gholami ⁶ and Chin Wei Lai ^{7,*}

¹ Department of Endodontics, Dental School, Shiraz University of Medical Sciences, Shiraz 7195615787, Iran

² Dentist, Dental School, Shiraz University of Medical Sciences, Shiraz 7195615787, Iran

³ Department of Chemical Engineering, National Taiwan University of Science and Technology, Taipei 106335, Taiwan

⁴ Nanomaterials and Polymer Nanocomposites Laboratory, School of Engineering, University of British Columbia, Kelowna, BC V1V 1V7, Canada

⁵ Oral and Dental Disease Research Center, School of Dentistry, Shiraz University of Medical Sciences, Shiraz 7195615787, Iran

⁶ Biotechnology Research Center, Shiraz University of Medical Sciences, Shiraz 7146864685, Iran

⁷ Nanotechnology and Catalysis Research Centre (NANOCAT), Institute for Advanced Studies (IAS), University of Malaya (UM), Kuala Lumpur 50603, Malaysia

* Correspondence: mousavi.nano@gmail.com (S.M.M.); cwlai@um.edu.my (C.W.L.)

Abstract: The undesirable side effects of conventional chemotherapy are one of the major problems associated with cancer treatment. Recently, with the development of novel nanomaterials, tumor-targeted therapies have been invented in order to achieve more specific cancer treatment with reduced unfavorable side effects of chemotherapeutic agents on human cells. However, the clinical application of nanomedicines has some shortages, such as the reduced ability to cross biological barriers and undesirable side effects in normal cells. In this order, bioinspired materials are developed to minimize the related side effects due to their excellent biocompatibility and higher accumulation therapies. As bioinspired and biomimetic materials are mainly composed of a nanometric functional agent and a biologic component, they can possess both the physicochemical properties of nanomaterials and the advantages of biologic agents, such as prolonged circulation time, enhanced biocompatibility, immune modulation, and specific targeting for cancerous cells. Among the nanomaterials, asymmetric nanomaterials have gained attention as they provide a larger surface area with more active functional sites compared to symmetric nanomaterials. Additionally, the asymmetric nanomaterials are able to function as two or more distinct components due to their asymmetric structure. The mentioned properties result in unique physicochemical properties of asymmetric nanomaterials, which makes them desirable materials for anti-cancer drug delivery systems or cancer bio-imaging systems. In this review, we discuss the use of bioinspired and biomimetic materials in the treatment of cancer, with a special focus on asymmetric nanoparticle anti-cancer agents.

Keywords: cancer; bioinspired nanomedicine; biomimetic materials; targeted drug delivery; asymmetry



Citation: Ghahramani, Y.; Mokhberi, M.; Mousavi, S.M.; Hashemi, S.A.; Fallahi Nezhad, F.; Chiang, W.-H.; Gholami, A.; Lai, C.W. Synergistically Enhancing the Therapeutic Effect on Cancer, via Asymmetric Bioinspired Materials. *Molecules* **2022**, *27*, 8543. <https://doi.org/10.3390/molecules27238543>

Academic Editors: Ioana Demetrescu and Andreea Didilescu

Received: 4 November 2022

Accepted: 1 December 2022

Published: 4 December 2022

Publisher's Note: MDPI stays neutral with regard to jurisdictional claims in published maps and institutional affiliations.



Copyright: © 2022 by the authors. Licensee MDPI, Basel, Switzerland. This article is an open access article distributed under the terms and conditions of the Creative Commons Attribution (CC BY) license (<https://creativecommons.org/licenses/by/4.0/>).

1. Introduction

Cancer is a term that encompasses a variety of diseases caused by the uncontrolled growth of malignant cells that can invade and spread to other parts of the body. The World Health Organization estimates that there will be 13.1 million cancer-related deaths by 2030, with more than 10 million new cases reported each year [1,2]. For both genders, lung cancer is the most commonly diagnosed cancer and the leading cause of cancer deaths. Breast cancer, prostate cancer, and colorectal cancer are other cancers commonly diagnosed in women [3]. The survival rate of cancer patients has been ameliorated with the development of an understanding of cancer physiology and its treatment modalities,

such as chemotherapy, radiotherapy, and immunotherapy. However, due to the lack of tumor specificity of these treatment methods, they can induce off-target side effects in healthy tissues as well as limited efficacy due to insufficient drug concentration at the tumor sites [4–6]. Moreover, in the case of resistance to single therapies, using combination therapies is essential, which can increase the risk of lethal side effects. Additionally, some cancer drugs, such as radioisotopes, toxins, nucleic acids, or hydrophobic drugs, cannot be administered systemically. Therefore, in order to overcome the mentioned limitations, targeted drug delivery using nanocarriers has been developed (Figure 1). Specific targeting augments drug solubility and bioavailability, increases drugs' stability, and improves drug targeting and its concentration in the tumor site [7–10].

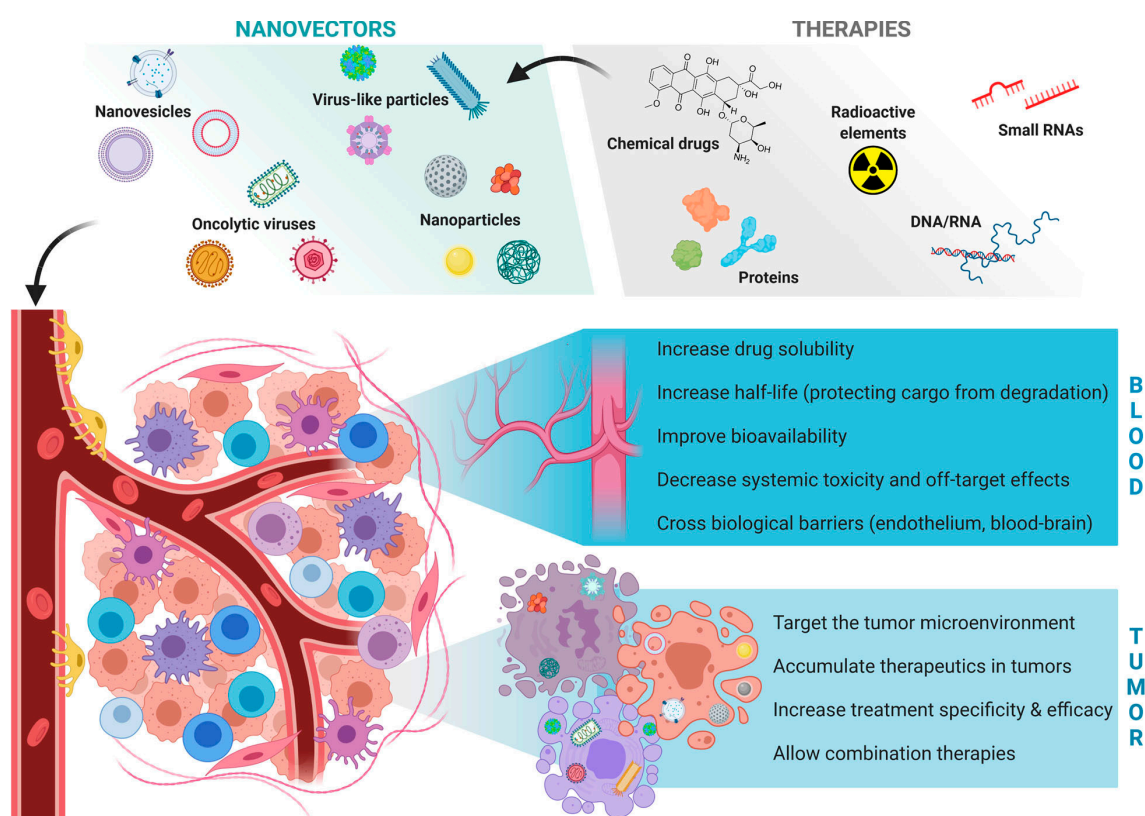


Figure 1. The advantages of applying nanocarriers for delivering cancer therapies [11].

Over the past few decades, different types of nanomaterials have been well developed for cancer therapies. The employed nanomaterials can be produced in symmetric or asymmetric structures. The nanomaterials are commonly synthesized in symmetric forms, such as nanospheres, nanowires, nanoflowers, or nanosheets. Additionally, after the discovery of Janus by Gennes et al. in 1991 [12], the asymmetric structures have gradually attracted increasing attention; thus, various asymmetric structures have been discovered in the last two decades. Nowadays, asymmetric structures contain various shapes with different surface properties [13–15]. Janus particles, bowl-shaped [16], snowman-shaped [17], disk-shaped [18], and raspberry-shaped structures [19], are examples of asymmetric nanomaterials. An asymmetric particle is a particle with an asymmetric center, similar to an asymmetric molecule. Different surface properties (e.g., charge, polarity, and chemical functionality) and particle shapes (e.g., dumbbells, snowmen, and Janus particles) can be responsible for the particle's asymmetry [20]. The application of nanomaterials in cancer therapy has various advantages due to their physicochemical properties, such as nanometric dimensions, large surface area-to-volume ratio, tunable surface characteristics, the ability to encapsulate various molecules, and controlled drug release [8,21–23]. Additionally, nanomedicine increases the therapeutic molecules' stability, bioavailability, and tumor

accumulation, resulting in a prolonged half-life in circulation compared to conventional chemotherapeutic drugs [24–27]. These properties make nanomedicines an excellent choice in tumor-targeted treatments. Despite the mentioned advantages and applications of nanomaterials in cancer therapy, some shortages are associated with these materials. In preclinical studies, the application of drug-loaded nanocarriers results in high drug concentrations in tumor sites with maximum therapeutic efficacy, while in clinical studies, the targeted synthetic nanoparticles (NPs) cannot work due to impenetrable biological barriers [8,28]. Therefore, scientists have been developing nanomedicine mimicking biological features with the inspiration of natural structures to overcome biological barriers. Additionally, synthetic nanomaterials can be modified with some biomimetic features. These bioinspired nanomedicines possess desirable properties such as excellent biocompatibility, proper biodegradation, and the ability to deliver high drug-loading content to target cells [29–31]. Therefore, bioinspired materials are a new solution to overcome biological barriers and the disadvantages of current drug delivery systems (DDSs). This review will discuss the application of asymmetric nanomaterials in cancer treatment.

2. Asymmetric Nanomaterials

As mentioned before, both symmetric and asymmetric structure nanomaterials are employed for cancer treatment. The symmetric structures (i.e., nanospheres, nanowires, nanoflowers, nanosheets, core-shell structured composites) are now commonly used in biomedical applications. Additionally, after the discovery of Janus by Gennes et al. in 1991 [12], the asymmetric structures have gradually attracted increasing attention; thus, various asymmetric structures have been discovered in the last two decades. Nowadays, asymmetric structures contain various shapes with different surface properties [13,32,33].

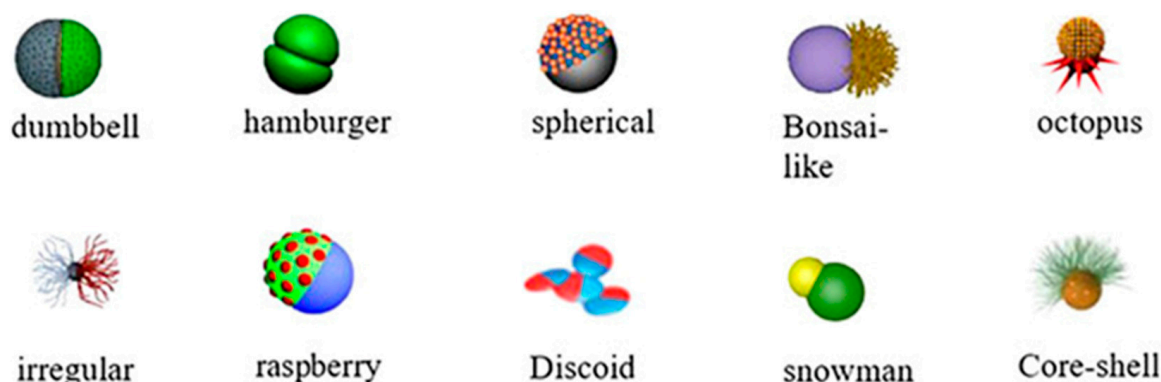
While the surface free energy effect limits symmetric structures, various unique advantages are related to asymmetric structures (Table 1). One of the most practical advantages of asymmetric structures is that they can possess multiple functions due to their different surface physiochemical properties or components. This results in the ability of these nanomaterials to simultaneously contain distinct properties (e.g., hydrophilicity and hydrophobicity), which makes the asymmetric structures ideal candidates for “nanointelligent systems” with desirable applications in biomedicine, electrochemistry, and interfacial stabilizers [13,34,35]. Furthermore, another advantage of asymmetric structures is a stronger synergistic effect. The distinct parts of asymmetric structures can perform independently or can even cooperate, resulting in enhanced efficiency. Additionally, because of their asymmetric shape, they have a larger effective surface area with an increased number of active sites, resulting in more preferred properties of these materials. Therefore, asymmetric materials have been widely developed in recent years due to their desirable properties [13]. Because of the interaction between asymmetric shapes and directional interactions, asymmetric particles with anisotropic features can yield more complex compositions than symmetric particles. The device usually has a symmetric geometry, and there is a limited amount of space available to load multiple drug types into the device. If two drugs are loaded simultaneously into a single storage space, the release of each drug cannot be independently controlled. In addition, the loaded multidrugs may interact adversely with each other, especially if the drugs have different chemical properties (e.g., hydrophilicity and hydrophobicity, acidity and basicity, etc.). Therefore, the development of multicompartiment carriers with independent storage sites to accommodate multiple drugs is urgently needed. Dual surface structures of an asymmetric nanostructure are anisotropic in composition, shape, and surface chemistry, which makes them ideal for binding dual guests to different domains of asymmetric particles. In addition, the functionally different surfaces of asymmetric particles can also be used for selective conjugation with specific triggers, allowing the release of the double guests to be individually controlled [36–38].

Table 1. The comparison of advantages and disadvantages between symmetric and asymmetric nanostructures.

Symmetric Structures	Asymmetric Structures
Lower effective surface area	Multiple functions
Fewer active sites	More active sites
Single function	Larger effective surface area
Free energy effect limits symmetric structures	Stronger synergistic effect
	Distinct properties
	Lower free energy
	More complex assemblies
	Increased number of unsaturated coordination centers
	More mechanic resistance
	Permeability

2.1. Janus Nanoparticles

Janus was the first asymmetric particle introduced by Pierre-Gilles Gennes in 1991 as a particle with two sides with opposite polarity [12]. With the development of nanotechnology, Janus nanoparticles (JNPs) are fabricated as NPs with two or more sides that have distinct chemical or physical properties. Generally, JNPs are divided into three groups due to their composition. JNPs can be organic (e.g., polymeric), inorganic (e.g., gold, silver, silica), or organic–inorganic [39–43]. Bowl-shaped [16], snowman-shaped [17], disk-shaped [18], raspberry-shaped [19], hamburger, spherical, bonsai-like, octopus, core-shell, and irregular structures [44] are the various shapes of JNPs (Figure 2).

**Figure 2.** The schematic illustration of some Janus nanoparticles [44].

Janus nanoparticles have attracted attention in cancer treatment due to their heterogeneous structure, as they can participate in two distinct functions. JNPs can incorporate various materials in order to achieve specific properties. As an example, with the incorporation of JNPs with imaging materials such as MnO_2 , Fe_3O_4 , gold and silver NPs, fluorescent dyes, or quantum dots, various imaging modalities are designed for tumor cell screening [45,46]. Several interesting properties can be obtained in nanoparticles with asymmetric heterostructural compounds at the micro/nanoscale that are not possible in homogeneous or symmetric nanostructures. For example, the Fe_3O_4 -Au JNPs exhibited magnetic properties on one side, while the Au NPs showed localized surface plasmon resonance on the other side. The Janus structure allowed Fe_3O_4 to be combined with Au, resulting in a different surface polarity or internal chemistry than the corresponding single components [47–49].

Moreover, incorporating JNPs with therapeutic agents can be employed as nanocarriers in various therapeutic modalities for cancer treatment, such as chemotherapy, phototherapy, radiotherapy, and gene therapy. In the drug delivery field, JNPs can be loaded with various distinct drugs with an independent release of multiple drugs [50], as well

as acting as nanomotors for active drug delivery or physical tumor destruction [51–53]. Therefore, the Janus nanoparticles have gained attention as the new nanoparticles in the cancer diagnosis and treatment era (Table 2).

2.1.1. Polymeric Janus Nanoparticles

In recent years, polymeric JNPs have been introduced as a drug delivery agent in cancer treatment. Janus dendrimers and spherical polymeric nanoparticles are the most common JNPs in drug delivery systems (DDS). Dendrimers are known as branched macromolecules with a core that is surrounded by repetitive branching units, known as “Dendron”. Janus dendrimers are a group of favorable drug carriers due to their properties, such as hydrophilicity, drug encapsulation ability, and the ability to conjugate with drugs with their abundant functional groups [54–56]. Dendrimers are categorized as asymmetric nanomaterials as they can have two or more distinct dendrons; thus, unlike symmetrical NPs, they can have more than one functional ability. As an example, Acton et al. fabricated polyethylene glycol (PEG)-based Janus dendrimers which can be loaded with two distinct hydrophobic and hydrophilic drugs. Additionally, the mentioned dendrimers are able to release the drugs at different speeds due to the different linkages between the dendrons and the drugs (Figure 3) [57–59].

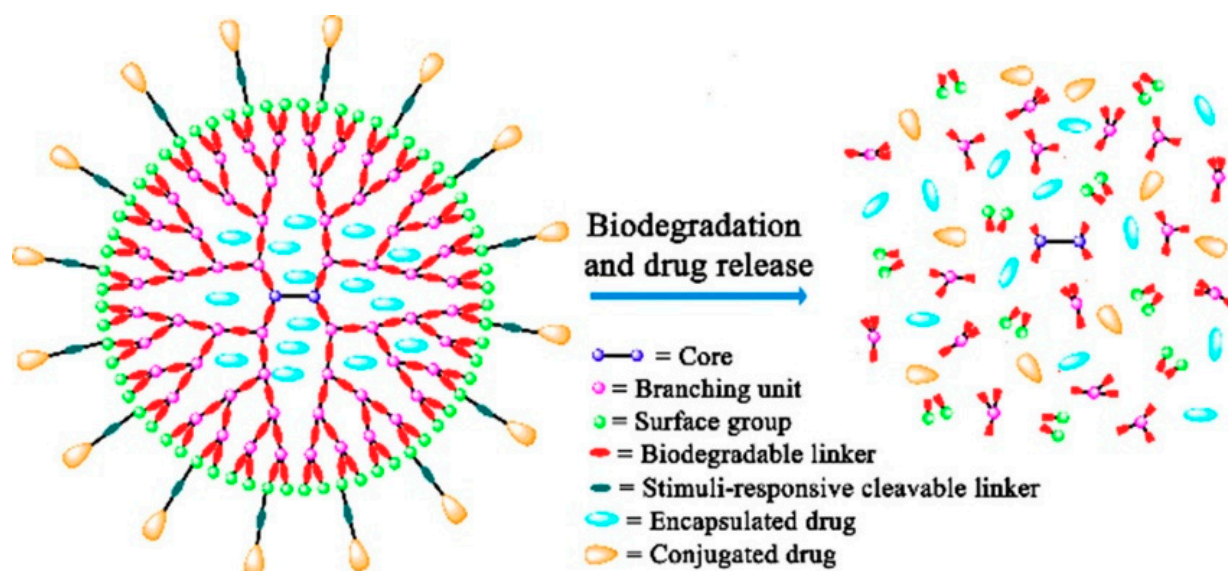


Figure 3. Schematic illustration of the biodegradation of biodegradable dendrimers [59].

The polymeric Janus materials are also applicable in cancer treatment. As the studies showed with the elimination of drug carriers in blood circulation by macrophages and neutrophils, polymeric Janus particles were introduced to overcome this problem. For instance, Sanchez et al. designed two-sided structures of polyethylene glycol (PEG) chains and Janus particles coupled with IgG, which reduced interference between the distinct functions of the two sides of JNPs by a spatial decoupling design of NPs, while the PEGs decrease the effect of macrophage evasion. Additionally, the mentioned study demonstrated that articles coated with only half PEG could escape from the immune system more effectively than particles coated with full PEG [60–62]. According to Xie and colleagues, biocompatible polymeric Janus nanoparticles composed of the FDA-approved polymer poly-(lactate-co-glycolic acid) (PLGA) can be prepared in one step using a fluidic nanoprecipitation system (FNPS). It was the first report of polymeric Janus nanoparticles capable of carrying a hydrophobic drug (paclitaxel) and a hydrophilic drug (doxorubicin hydrochloride) in a single particle [63,64].

2.1.2. Inorganic Janus Nanoparticles

Inorganic materials such as gold, silver, silica, MnO_2 , or Fe_3O_4 can be utilized in the fabrications of Janus nanoparticles for cancer diagnosis and treatment (Figure 4) due to their physicochemical properties such as magnetism, surface plasmonic resonance (SPR), photo-thermal conversion ability, and easy functionalization [65]. Therefore, the inorganic-based JNPs are mainly employed as cancer imaging agents in magnetic resonance imaging (MRI), magnetic particle imaging, computerized tomography (CT) scans, photoacoustic imaging processing (PAI), surface-enhanced Raman scattering (SERS), etc. [66]. In a study, Reguera et al. fabricated a star-shaped JNP that forms the initial Fe_3O_4 -Au dumbbell JNPs. The fabricated nanostar can be utilized in MRI, CT, SERS, or PAI cancer imaging systems [67–70].

In addition to imaging systems, inorganic JNPs are employed in various cancer treatment modalities. In a study, the surface of silica-based JNPs was functionalized with alkyne-tagged anti-CD28 and biotinylated anti-CD3 antibodies, fabricating bifunctional Janus nanoparticles. As a result, the fabricated JNPs can be utilized as T-cell stimulation NPs in immunotherapies against tumors, containing both anti-CD3 and anti-CD28 stimulatory ligands in two distinct sides of JNPs [71]. In another study, gold-mesoporous silica JNPs were designed and then modified with folic acid; thus, the fabricated JNPs can be employed as drug nanocarriers. In the mentioned study, the gold-mesoporous silica JNPs were loaded with doxorubicin (DOX) (an anti-cancer chemotherapy drug), which can be released from the mesoporous agents in a pH-sensitive manner, targeting and entering hepatocellular carcinoma tumor cells. In addition to chemotherapy, the gold-mesoporous silica JNPs can act both as radiotherapy and CT-scan agents due to the physicochemical properties of inorganic gold and silica molecules, as mentioned before [72,73].

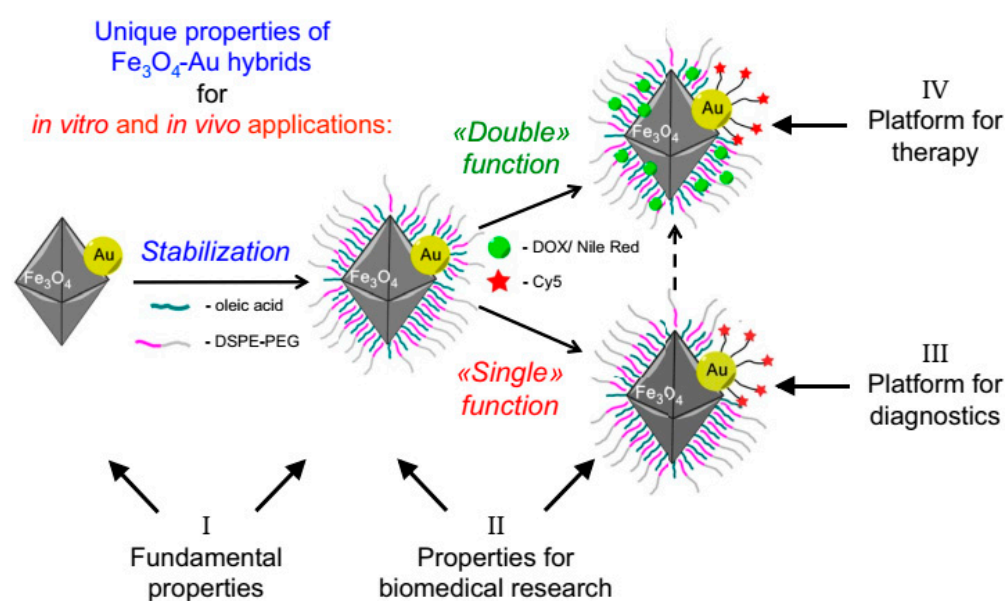


Figure 4. Schematic illustration of Au- Fe_3O_4 multifunctional Janus nanoparticles as a cancer diagnostic and therapeutic agent [74].

Despite the challenges facing molecular organic-inorganic hybrid mesoporous organosilica nanoparticles (MONs), the precise control of morphology, nanostructure, composition, and particle size remains a challenge. It has been shown that hollow MOS nanoparticles (HMONs) with uniform spherical morphology can be prepared using a hard template. An efficient growth strategy governed by bridged organic groups was proposed for the facile synthesis of highly dispersed and uniform MONs with different Janus morphologies, nanostructures, organic-inorganic hybrid compositions, and particle sizes. As long as the bridged organic groups and the concentration of bis-silylated organosilica precursors are varied, the properties of MONs can be easily controlled. In addition to their excellent

performances as stimuli-responsive drug carriers, adsorbents for bilirubin removal, and contrast agents for ultrasound imaging, Janus MONs have hollow structures [1,75].

2.1.3. Polymeric-Inorganic Janus Nanoparticles

In addition to polymeric and inorganic JNPs, a new category of Janus nanoparticles was also designed by combining these two mentioned JNPs, named polymeric-inorganic Janus nanoparticles. These JNPs are widely employed for biomedical applications, including cancer diagnosis and treatment. In a study, a polystyrene/ $\text{Fe}_3\text{O}_4@/\text{SiO}_2$ Janus nanocomposite was designed by Wang et al. for administering targeted drug delivery. The mentioned JNP was further loaded with folic acid on the polystyrene side and doxorubicin on the silica side [76–78]. Additionally, with the application of Fe_3O_4 nanoparticles, and due to their unique properties, simultaneous targeting, drug delivery, and imaging can be performed. In another study, gold-mesoporous silica Janus nanoparticles were employed in a bio-imaging system (Figure 5). In these multifunctional JNPs, the nanoparticles were designed to target hepatocellular Carcinoma due to the folic acid molecules in their structure. In other words, the folic acid modification of these JNPs enables them to act as targeted computed tomography (CT) and imaging agents for diagnosing hepatocellular Carcinoma [72,79].

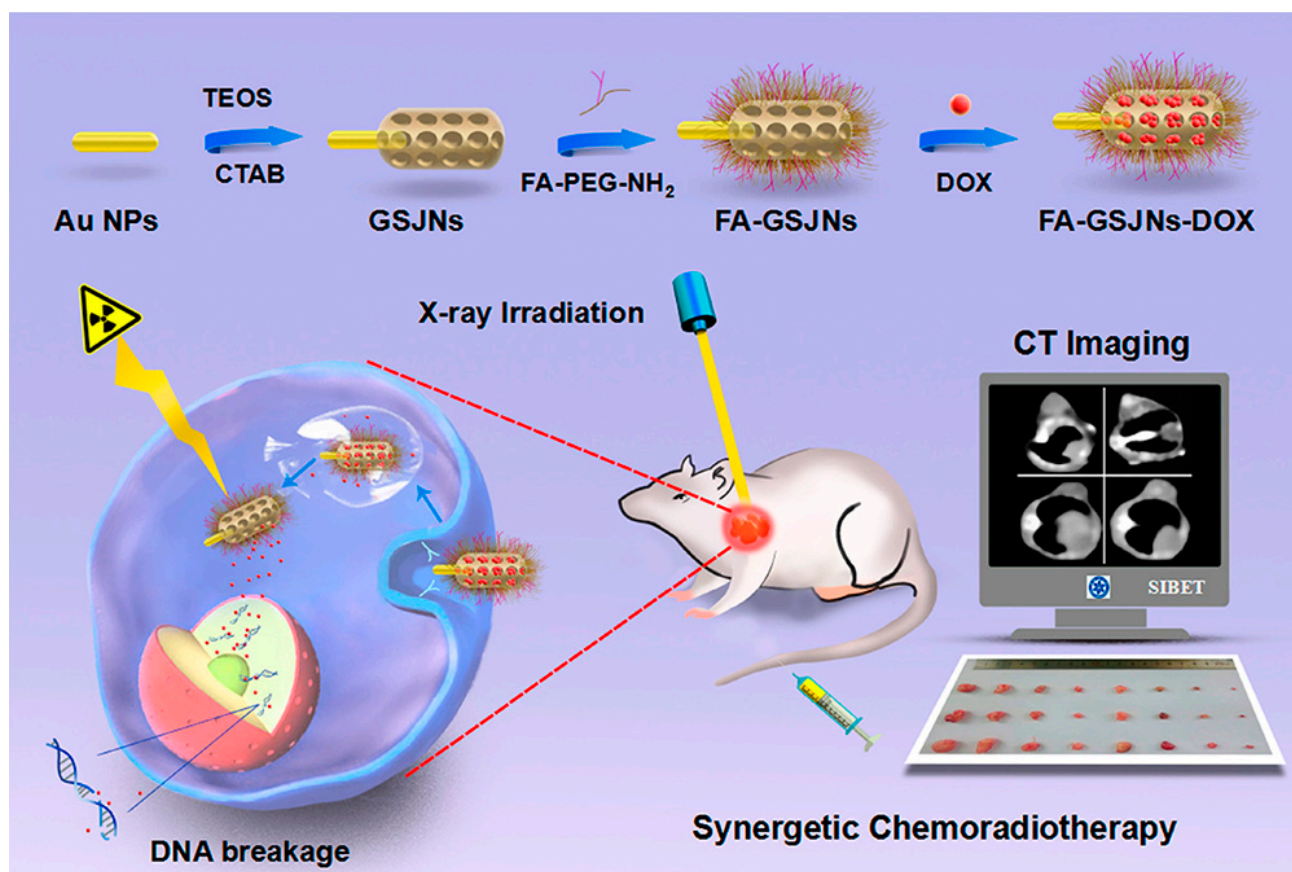


Figure 5. A multifunctional gold-mesoporous silica Janus nanoparticle designed for a bio-imaging system [72].

Table 2. The examples of employed JNPs in the studies related to cancer diagnosis and treatments.

Type	Composition	JNPs Morphology	Application	Reference
Organic	Four PEG-based dendrons	Dendrimers	Chemotherapy	[57]
Inorganic	PLGA nanoparticles-DOX-PTX	Sphere	Chemotherapy	[63]
	Silica-antibodies	Sphere	Immunotherapy	[71]
	Fe ₃ O ₄ -Au	Octahedron-sphere/Star	CT, MRI, Chemotherapy, PIA, SERS	[67,74]
	Au-silica	Sphere	PIA	[80]
	FA-Au-mesoporous silica-DOX	Spindle	CT, Chemotherapy, Radiotherapy	[72]
	GNRs@mSiO ₂ -DOX	Lollipop	Chemotherapy	[81]
	FA-Au/Fe ₃ O ₄ @C	Dumbbell	MRI, CT, Chemotherapy	[82]
	DOX-CMR-MS/Au-6MP	Dumbbell	Chemotherapy, SERS	[83]
	Fe ₃ O ₄ -MSNs-P@GCV@pTK	Rod	MRI, Magnetic hyperthermia, Gene therapy	[84]
	Fe ₃ O ₄ -SiO ₂	Bullet	Magnet field-enhanced chemotherapy	[85]
	Ag-MSN-DOX	Bullet	Chemotherapy	[86]
	Fe ₃ O ₄ -PS16-PAA10	Sphere	Chemotherapy	[87]
	FA-Polystyrene/Fe ₃ O ₄ @SiO ₂ -DOX	Sphere	Chemotherapy	[87]
	Au-polydivinylbenzene-curcumin	Sphere	Chemotherapy	[88]
FA-Au-PAA/mCaP	Dumbbell	CT, Chemotherapy	[89]	

2.2. Asymmetric Mesoporous Materials

Mesoporous materials are materials with 2–50 nm diameter pores, which have been widely developed over the past decades [80,90,91]. The first mesoporous materials were bulk, but with their increased application in various fields, nano-sized mesoporous materials were fabricated, known as mesoporous nanoparticles [92–94]. Nowadays, mesoporous NPs are widely employed in various domains, including biomedicine and drug delivery, due to their large surface area, high pore volume, and tunable pore size, with various structures and components. The mesoporous NPs are fabricated in unique symmetric and asymmetric architectures, as shown in Figure 6.

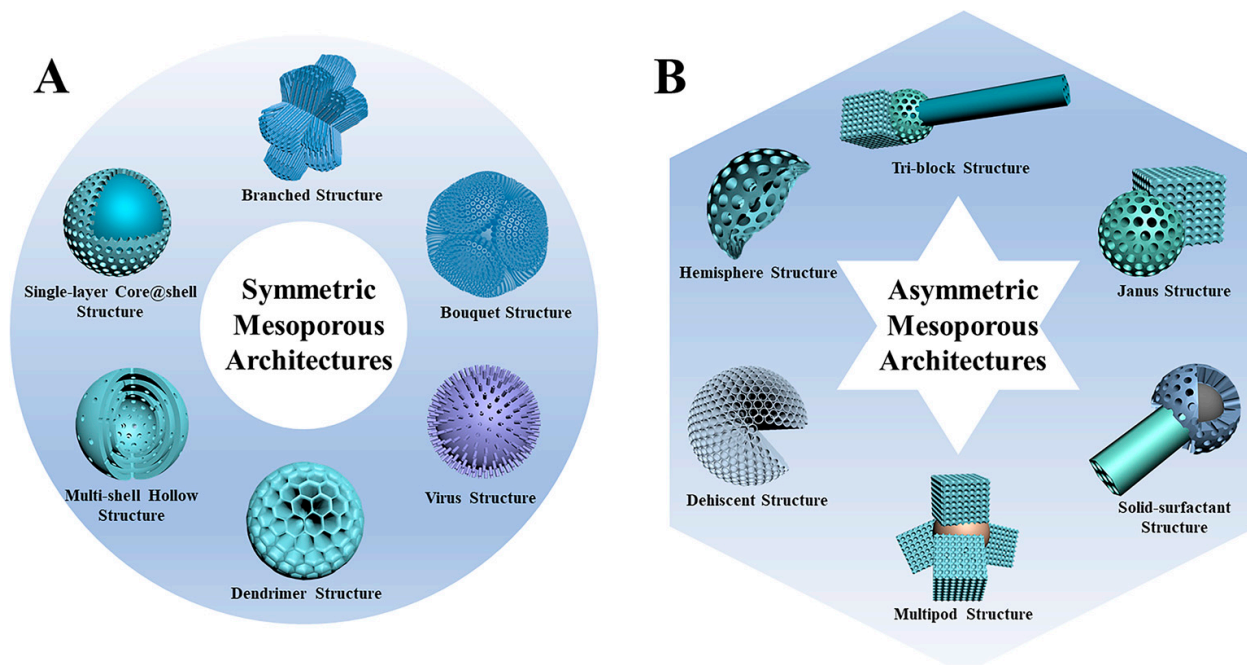


Figure 6. Schematic illustrations of (A) symmetric and (B) asymmetric mesoporous nanoparticles with various architectures [95].

Despite the symmetric NPs, asymmetric mesoporous NPs are designed for multiple-component drug-loading systems or ligand attachment due to having more than one distinct structure. Moreover, each mesoporous component can contain different pore sizes, particle sizes, electric charges, hydrophilicity, etc.; therefore, each component is able to

interact independently with the surrounding environment. This characteristic makes the asymmetric mesoporous nanoparticles a favorable material for biomedical applications and drug delivery systems. In a study, Li et al. fabricated multifunctional asymmetric UCNP@SiO₂@mSiO₂&PMO (UCNP = upconversion nanoparticle, PMO = periodic mesoporous organosilica) nanoparticles. These NPs contain a hydrophilic side (mSiO₂) and a hydrophobic side (PMO); therefore, the NPs can be loaded with hydrophilic doxorubicin drugs on the mSiO₂ side, and with the hydrophobic paclitaxel molecules on the PMO side. These two drugs can be released independently due to heat production with NIR light [36]. Mesoporous silica nanoparticles with anisotropic geometry and dual compartments are highly desirable for loading and unloading dual drugs in segregated storage environments. An anisotropic epitaxial growth strategy has successfully developed an asymmetric lollipop-shaped mesoporous silica nanoparticle Fe₃O₄@SiO₂&EPMO (EPMO = ethane-bridged periodic mesoporous organosilica). An asymmetric nanoparticle exhibits a uniform lollipop shape with a 200 nm diameter spherical core of iron₃O₄@SiO₂ and a 90 nm-long EPMO nanorod with a specific surface area of 650.3 square meters g⁻¹. According to *in vitro* studies, the asymmetric nanoparticles possess a unique dual independent (hydrophilic/hydrophobic) space design with high loading capacity and are significantly more effective than pure drugs at killing cancer cells. In addition, the dual drug-loaded nanoparticles (curcumin plus gentamicin sulfate) exhibited excellent antibacterial and anticancer properties [96–98].

The asymmetric nanoparticles of mesoporous silica have a head-to-tail structure and are potent immunoadjuvants capable of delivering peptide antigens to mice and eliciting greater antibody immune responses than their symmetric counterparts. According to Abbaraju et al., asymmetric mesoporous silica nanoparticles with a head-to-tail morphology (HTMSN) were more effective than symmetric mesoporous silica nanoparticles (MSN) when using a peptide antigen as an adjuvant. Recently, it has been reported that HTMSNs have been synthesized and have the potential to be used as an adjuvant *in vitro*. To demonstrate the efficacy of HTMSNs as vaccine adjuvants, researchers used J8 (molecular weight 3283) as a model antigen that can be efficiently loaded in both MSNs and HTMSNs. The J8 peptide, developed from the bacterial surface M protein, generates antibody-specific immunity and protection against *Streptococcus pyogenes* (SP), an infection known for its numerous clinical manifestations, including toxic shock syndrome, rheumatic fever, and rheumatic heart disease (RHD). In studies using MSN and HTMSN as both the adjuvant and carrier, HTMSN showed enhanced uptake into antigen-presenting cells (APCs) and the increased activation of costimulatory molecules (e.g., CD40, CD86) on the surface of matured APCs compared with MSN. Another study in mice found that HTMSN loaded with J8 elicited a stronger response to J8-specific antibodies than MSN [99,100]. In another study, asymmetric single-hole mesoporous silica nanocages were designed. These nanoparticles are hollow spheres of 100–240 nm diameter, with mesoporous shells on the surface area. These NPs can be loaded with drugs of various sizes, due to their central hollow area (~25 nm) and the mesopores in silica molecules with 2–10 nm diameter. In this study, the mesoporous silica NPs were loaded with both bovine serum albumin and doxorubicin, with two different particle sizes. These molecules can also be released separately, controlled by heat and NIR light [101–103].

3. Core–Shell Nanoparticles

Core–shell nanoparticles are a type of asymmetric nanoparticles with distinct components in an inner core and outer shell, which makes this nanoparticle able to attach to both nanometric and micrometric scales. More importantly, their particular structure results in a controlled releasing action while protecting the drug molecules. Due to their application and purpose, core–shell NPs can be fabricated in different core shapes, shell structures and thicknesses, and surface properties. The mentioned characteristics can determine the loading capacities and releasing kinetics of drugs. The core–shell NPs usually vary between

10–200 nm, as the smaller particles will be inactivated by immune cells, and the larger ones will be recognized as foreign body particles, causing inflammation [104,105].

Various core–shell nanoparticles have been employed successfully as anti-cancer drug delivery agents. In the studies, magnetic NPs, gold NPs, Fe_3O_4 , and other conducting NPs are mainly used as core materials. As an example, Ayyanaar et al. employed Fe_3O_4 nanoparticles as the core material, coated in poly(lactic-co-glycolic acid) (PLGA) mesoporous molecules, fabricating PLGA- Fe_3O_4 nanoparticles. These nanoparticles were loaded with curcumin which is an anti-cancer agent [106].

4. The Applications of Asymmetric Nanomaterials in Cancer Treatment

As mentioned, asymmetric structures are employed for various applications due to their desirable properties, such as a more significant surface area, increased active sites, and tunable structures and compositions. Among the nanomaterials, carbon-based and silica-based asymmetric nanomaterials have been widely developed recently due to their advantages, such as favorable biocompatibility, facile application, and structural adjustability [29,107]. Additionally, asymmetric nanomaterials have been designed for biomedical applications because of their ability to integrate different functional components, structures, and even properties. In this regard, this section will thoroughly discuss the application of asymmetric nanomaterials in cancer treatment.

4.1. Drug Delivery

Enhancing drug delivery systems (DDS) is one of the significant applications of asymmetric nanomaterials in cancer treatment. The tumor-targeted drug delivery of anti-cancer drugs has been developed in past decades to achieve a controlled drug-releasing system to increase the treatment efficacy and decrease the off-target effects. Nanomaterials are considered favorable drug carriers in cancer therapy. In addition, asymmetric nanomaterials are more efficient as their distinct components can function separately. For example, Shao et al. designed a bullet-like nanoparticle (NP) with a head of Fe_3O_4 and a body of mesoporous silica [85,108]. In this nanoparticle, the magnetic Fe_3O_4 enables an increased drug concentration and enhanced cellular uptake using magnetic field-guided tumor accumulation. Additionally, the mesoporous silica enables the enhanced loading of the drugs. Moreover, the mentioned NP can be loaded with various molecules. The Janus Fe_3O_4 –mesoporous silica NP can be loaded with photosensitizers for combination therapies, while Fe_3O_4 is used for inducing magnetic hyperthermia combined with the photodynamic therapy of tumor cells to prevent metastasis [109]. In addition, the metallic part can be replaced by gold or silver NPs for reaching synergistic photo-thermal/chemotherapy applications due to the photo-thermal properties of noble NPs [110–112]. In another study, octopus-type gold nanostar-mesoporous silica asymmetric NPs were utilized. The silica segments of these NPs were conjugated with lactobionic acid (LA). This conjugation induces a higher drug capacity of the NPs, with affected drug release properties by pH and near-infrared (NIR), resulting in actively targeted chemo-photothermal therapy [113]. Moreover, asymmetric NPs are advantageous in cargo delivery. The conventional NPs do not have enough drug-loading capacity for large biomolecules like nucleic acids and proteins, while asymmetric NPs have higher cargo-loading efficiency. In a study, Qiao et al. designed bowl-shaped silica NPs with high loading capacity for plasmid DNA, applicable for DNA delivery systems [114,115].

In order to reach efficient drug delivery, the cellular uptake of these nanocarriers is also important. A suggested solution for increasing cellular uptake is using a rough surface head component. In the study by Li et al., they developed asymmetric nanotruck NPs with rough silica and a periodic mesoporous organosilica (PMO) rod, resulting in the enhanced intracellular uptake of the nanotruck compared to smooth-surfaced PMO [90]. Additionally, the upconverting nanoparticles (UCNPs) can be encapsulated with a rough silica head for a dual application of bio-imaging and NIR-triggered drug delivery [13]. This specific design

suggests the potential of achieving various distinct applications for a single nanoparticle by developing new structural properties in asymmetric NPs.

In addition, the unique properties of the asymmetric NPs make it possible to tailor them for a particular application like dual drug delivery. As an example, a dual-component asymmetric NP was developed by Zhao et al., using mesoporous silica and PMO for dual-drug delivery. Since mesoporous silica is hydrophilic and PMO is a hydrophobic component, this NP can be loaded with two hydrophilic and hydrophobic drugs without interfering [36,116]. Additionally, the outer surface of the asymmetric NPs can be modified with different functional groups. López et al. designed asymmetric Janus mesoporous silica particles with two different targeted ligands. One is a folic acid molecule for binding to the folate receptors of the cell membrane, and the other is triphenylphosphine for binding to the mitochondria membrane. This unique design results in a higher nanoparticle concentration inside the tumor cells due to folic acid ligands with the guided transportation of nanocarriers near the mitochondria with triphenylphosphine function [117]. This asymmetric designing strategy facilitates the targeted delivery of NPs from cell to organelle compared to conventional symmetric NPs. (Figure 7).

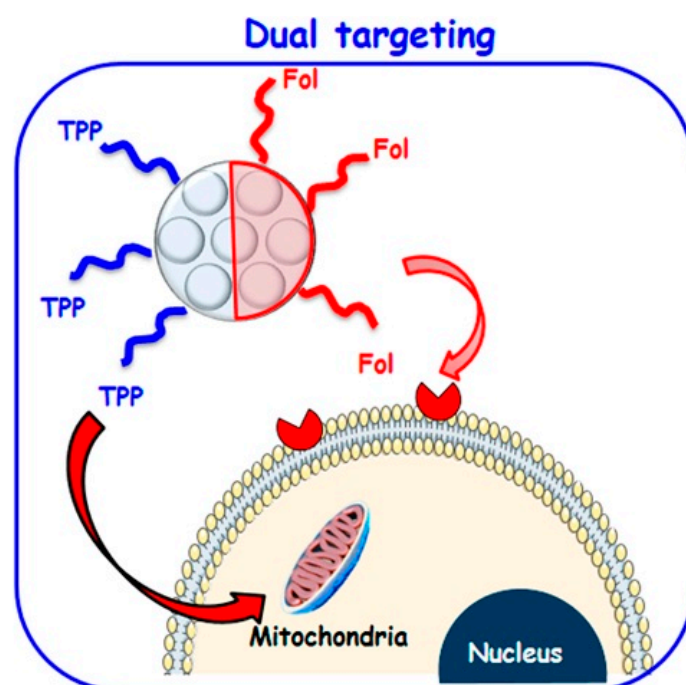


Figure 7. Dual targeting strategy to attack both tumor cell membrane and mitochondria by asymmetrically functionalized nanoparticles [118].

The asymmetric nanoparticles also apply in active drug delivery systems using nanomotors. The asymmetric structures with tunable properties enable the nanomotors to move in complex biological conditions to achieve efficient drug delivery. The studies suggest that the asymmetric silica-based motors can significantly penetrate cell membranes or tumor cells due to the autonomous motion of these nanomotors [119–123].

4.2. Tumor Imaging Systems

After the production of cancer cells in the human body, they can replicate rapidly, resulting in tumor formation. Additionally, these cancerous cells can transfer through the circulation system and metastasis in various organs. Therefore, developing tumor screening systems for the early detection of tumoral cells is essential. With the development of nano-materials' applications in biomedicine, they are widely employed for tumor detection by various screening modalities such as biosensors, multifunctional CT scans, or MRI systems.

Like other nanometric materials, asymmetric nanoparticles are also employed for tumor detection. Gold-integrated asymmetric NPs have great potential for application in radiosensitization and the computerized tomography (CT) imaging of tumors [72,124]. In a study, Wang et al. designed a carbon-based snowman-shaped asymmetric nanostructure with gold and Fe_3O_4 , resulting in simultaneous CT/magnetic resonance imaging (MRI) and chemo-photothermal synergistic therapy in a single asymmetric nanostructure [82,125].

Detecting cancer biomarkers with biosensors is another method of tumor detection. Nanomaterials are commonly used in the structure of biosensors. As nanomaterials have high electrical conductivity, high affinity to biomolecules, and high surface area-to-weight ratios, they are known as desirable candidates in biosensor fabrication. The application of nanomaterials can optimize the signal transduction of biosensors due to the enhancement of sensitivity [126,127]. Therefore, it has resulted in the better selectivity of biomolecules, signal/noise ratio, and signal per effect due to multiple receptors, as well as decreasing the size of the electrochemical biosensors [128–131]. Designing the ideal electrode with high selectivity and sensitivity is a significant limitation of the biosensors, which conjugating NPs resolve to the biomarkers [132]. Additionally, choosing the proper functional group is essential for an ideal biosensor design. As mentioned, asymmetric NPs can bind with various molecules or modify with distinct functional groups due to their unique physical properties. Therefore, asymmetric nanomaterials can be utilized in the designing and production of cancer biosensors in order to achieve enhanced detection selectivity and specificity.

5. Bioinspired and Biomimetic Nanomaterials in Cancer Therapy

Despite the advantages of the nanoparticles in the targeted drug delivery systems, they contain low drug delivery efficacy due to improper biocompatibility and low permeability in biological barriers; thus, bioinspired and biomimetic nanomaterials are developed in recent years to overcome these shortages, resulting in higher bioavailability and an enhanced therapeutic effect. In this section, one of the most common bio-inspired materials in cancer therapy will be discussed. Among the vitamins, Vitamin B12 (VB12) is an ideal material for NP production. VB12 has receptor-mediated endocytosis in the human body and forms a complex with the intrinsic stomach matrix. For instance, Chalasani et al. designed a study in which the drug availability of covalent conjugation of VB12 to insulin-loaded dextran was compared with pure NPs. The results of this study indicated the higher pharmacological availability of VB12-conjugated drugs [133,134].

Vitamin B9, also known as folic acid (FA), is another vitamin with a significant affinity for folate receptors, resulting in an increased cellular uptake of tumor cells. In a study, a polystyrene/ Fe_3O_4 @ SiO_2 Janus nanocomposite was designed by Wang et al. for administering targeted drug delivery. The JNP was loaded with folic acid on the polystyrene and doxorubicin on the silica side [76,135]. In another study, gold-mesoporous silica Janus nanoparticles were employed in a bio-imaging system. In these multifunctional JNPs, the nanoparticles were designed to target hepatocellular carcinoma due to the folic acid molecules in their structure. In other words, the folic acid modification of these JNPs makes it possible to act as targeted computed tomography (CT) and imaging agents for diagnosing hepatocellular carcinoma [72]. In another study, López et al. designed asymmetric Janus mesoporous silica particles with two targeted ligands. One is a folic acid molecule for binding to folate receptors of the cell membrane, and the other is triphenylphosphine for binding to the mitochondria membrane. The folic acid ligands facilitate the guided transportation of nanocarriers near the mitochondria, a higher nanoparticle concentration inside the tumor cells [117,136]. This asymmetric designing strategy facilitates the targeted delivery of NPs from cell to organelle compared to conventional symmetric NPs.

Furthermore, in a study by Yang et al., the asymmetric folic acid-coated chitosan NPs were employed as polymeric NPs in the oral cancer imaging system. The fabricated NPs have an excellent capacity for drug loading and an enhanced drug release in cellular

lysosomes. In the NP structures, the folic acid ligands facilitate the endocytosis of NPs by attaching to folate receptors on the oral cancer cells [137,138].

6. Future Perspective

In this review, various bioinspired nanomaterials for cancer treatments were discussed. Despite the various experimental studies performed on these nanomaterials, only a few clinical studies were performed; therefore, further clinical investigations are needed in order to confirm the advantages and efficacy of these materials in the clinic. Furthermore, these materials mostly have complicated structures with time-consuming and costly production, inhibiting their commercialized production. Additionally, in clinical treatment, high drug concentration in target cells and efficient drug release are needed; therefore, combination therapies must be introduced to increase the affectivity of DDS. For example, ultrasound-guided drug delivery can be a promising method for combined targeted drug delivery, with the utilization of the thermal and mechanical effects of the ultrasound on the employed nanomaterials.

As discussed in this article, asymmetric nanomaterials are widely used in cancer treatment; however, they are just in the primary stages of development and still need to overcome their shortages. First, there is a need to explore an efficient system for fabricating these asymmetric materials on industrial scales. Additionally, some of the asymmetric nanomaterials are currently fabricated in simple asymmetric structures, such as bowl-shaped structures; thus, it is critical to develop methods for the facile and efficient production of these materials in more complex structures and functions. Similar to bioinspired materials, producing asymmetric NPs is also very expensive. Therefore, it is essential to develop efficient and cost-effective methods for fabricating these asymmetric nanomaterials on industrial scales in order to use them in cancer treatments.

7. Conclusions

One of the major problems of conventional cancer therapies is their off-target effects on healthy tissues. Recently, with the development of novel nanomaterials, tumor-targeted therapies have been invented in order to achieve more specific cancer treatment with reduced unfavorable side effects of chemotherapeutic agents on human cells. In this review, we tend to discuss the application of nanomaterials in cancer treatment, emphasizing asymmetric nanomaterials due to their advantages in drug delivery systems, as they can possess multiple functions due to their different surface physiochemical properties or different components. However, the clinical application of nanomedicines has various disadvantages, such as the reduced ability to cross biological barriers and undesirable off-target effects. In this order, the bioinspired materials are developed to minimize the related side effects due to their excellent biocompatibility and higher accumulation therapies. Therefore, this article discussed the asymmetric bioinspired and biomimetic nanomaterials in cancer treatments.

Author Contributions: Y.G. and S.A.H. developed the idea and structure of the review article. M.M. wrote the manuscript and collected the materials from databases. S.M.M., A.G., F.F.N. and W.-H.C. wrote, revised, and improved the manuscript. S.M.M. and C.W.L. supervised the manuscript. All authors have read and agreed to the published version of the manuscript.

Funding: This research work was financially supported by the Fundamental Research Grant Scheme FRGS/1/2020/TK0/UM/02/8 (No. FP023-2020), and Global Collaborative Programme—SATU Joint Research Scheme (No. ST004-2021).

Institutional Review Board Statement: Not applicable.

Informed Consent Statement: Not applicable.

Data Availability Statement: All data generated or analyzed during this study are included in this published article.

Conflicts of Interest: The authors declare no conflict of interest.

Abbreviations

5 FU: 5 fluorouracil; BC: Bacterial Cellulose; BPPE: black pomegranate peel extract; CCMNPs: chitosan-coated magnetic nanoparticles; CD: Cyclodextrins; CDDP: cis diamminedichloroplatinum; CNPs: covalent channel-type nanoparticles; CT; computerized tomography; DDSs: drug delivery systems; DOX: doxorubicin; EGFR: growth factor receptor; FA: folic acid; FGB: Folic acid-gold-bilirubin; JNPs: Janus nanoparticles; LA: lactobionic acid; M- γ -CD: mannose-modified γ -cyclodextrin; MRI: magnetic resonance imaging; MNPs: Magnetic nanoparticles; NIR: near-infrared; NPs: nanoparticles; OSCC: oral squamous cell carcinoma; PAI: photoacoustic imaging processing; PCL: polycaprolactone; PEG: polyethylene glycol; PEI: polyethyleneimine; PGA: poly (glycolic acid); PLA: poly (lactic acid); PLGA: poly (lactic-co-glycolic acid); PMO: periodic mesoporous organosilica; SERS: surface-enhanced Raman scattering; SPR: surface plasmonic resonance; RES: reticuloendothelial system; RG: Regorafenib ROS: reactive oxygen species; TiO₂: titanium dioxide; UCNPs: upconverting nanoparticles; VB12: Vitamin B12; VLPs: Virus-Like Particles.

References

1. Tao, G.; Bai, Z.; Chen, Y.; Yao, H.; Wu, M.; Huang, P.; Yu, L.; Zhang, J.; Dai, C.; Zhang, L. Generic synthesis and versatile applications of molecularly organic–inorganic hybrid mesoporous organosilica nanoparticles with asymmetric Janus topologies and structures. *Nano Res.* **2017**, *10*, 3790–3810. [[CrossRef](#)]
2. Mousavi, S.-M.; Nejad, Z.M.; Hashemi, S.A.; Salari, M.; Gholami, A.; Ramakrishna, S.; Chiang, W.-H.; Lai, C.W. Bioactive agent-loaded electrospun nanofiber membranes for accelerating healing process: A review. *Membranes* **2021**, *11*, 702. [[CrossRef](#)] [[PubMed](#)]
3. Mohamed Isa, E.D.; Ahmad, H.; Abdul Rahman, M.B.; Gill, M.R. Progress in mesoporous silica nanoparticles as drug delivery agents for cancer treatment. *Pharmaceutics* **2021**, *13*, 152. [[CrossRef](#)]
4. Landgraf, M.; Lahr, C.A.; Kaur, I.; Shafiee, A.; Sanchez-Herrero, A.; Janowicz, P.W.; Ravichandran, A.; Howard, C.B.; Cifuentes-Rius, A.; McGovern, J.A. Targeted camptothecin delivery via silicon nanoparticles reduces breast cancer metastasis. *Biomaterials* **2020**, *240*, 119791. [[CrossRef](#)]
5. Azhdari, R.; Mousavi, S.M.; Hashemi, S.A.; Bahrani, S.; Ramakrishna, S. Decorated graphene with aluminum fumarate metal organic framework as a superior non-toxic agent for efficient removal of Congo Red dye from wastewater. *J. Environ. Chem. Eng.* **2019**, *7*, 103437. [[CrossRef](#)]
6. Mousavi, S.M.; Behbudi, G.; Gholami, A.; Hashemi, S.A.; Nejad, Z.M.; Bahrani, S.; Chiang, W.-H.; Wei, L.C.; Omidifar, N. Shape-controlled synthesis of zinc nanostructures mediating macromolecules for biomedical applications. *Biomater. Res.* **2022**, *26*, 4. [[CrossRef](#)] [[PubMed](#)]
7. Bjornmalm, M.; Thurecht, K.J.; Michael, M.; Scott, A.M.; Caruso, F. Bridging bio–nano science and cancer nanomedicine. *ACS Nano* **2017**, *11*, 9594–9613. [[CrossRef](#)] [[PubMed](#)]
8. Shi, J.; Kantoff, P.W.; Wooster, R.; Farokhzad, O.C. Cancer nanomedicine: Progress, challenges and opportunities. *Nat. Rev. Cancer* **2017**, *17*, 20–37. [[CrossRef](#)] [[PubMed](#)]
9. Bahrani, S.; Hashemi, S.A.; Mousavi, S.M.; Azhdari, R. Zinc-based metal–organic frameworks as nontoxic and biodegradable platforms for biomedical applications: Review study. *Drug Metab. Rev.* **2019**, *51*, 356–377. [[CrossRef](#)]
10. Mousavi, S.M.; Farsi, M.; Azizi, M. Enhancement of rheological and mechanical properties of bitumen using styrene acrylonitrile copolymer. *J. Appl. Polym. Sci.* **2015**, *132*, 41875. [[CrossRef](#)]
11. Briolay, T.; Petithomme, T.; Fouet, M.; Nguyen-Pham, N.; Blanquart, C.; Boisgerault, N. Delivery of cancer therapies by synthetic and bio-inspired nanovectors. *Mol. Cancer* **2021**, *20*, 55. [[CrossRef](#)] [[PubMed](#)]
12. de Gennes, P. Ecole Supérieure de Physique et de Chimie/industrielles de la Ville de Paris, 70 rue Vauguelin, Paris Cedex 05, France. *Rev. Mod. Phys.* **1992**, *64*, 75237.
13. Li, H.; Chen, L.; Li, X.; Sun, D.; Zhang, H. Recent Progress on Asymmetric Carbon-and Silica-Based Nanomaterials: From Synthetic Strategies to Their Applications. *Nano-Micro Lett.* **2022**, *14*, 45. [[CrossRef](#)] [[PubMed](#)]
14. Brazesh, B.; Mousavi, S.M.; Zarei, M.; Ghaedi, M.; Bahrani, S.; Hashemi, S.A. Biosorption. In *Interface Science and Technology*; Elsevier: Amsterdam, The Netherlands, 2021; Volume 33, pp. 587–628.
15. Mousavi, S.M.; Hashemi, S.A.; Bahrani, S.; Mosleh, S.; Chiang, W.-H.; Yousefi, K.; Ramakrishna, S.; Wei, L.C.; Omidifar, N. Hybrid of sodium polytungstate polyoxometalate supported by the green substrate for photocatalytic degradation of auramine-O dye. *Environ. Sci. Pollut. Res.* **2022**, *29*, 56055–56067. [[CrossRef](#)] [[PubMed](#)]
16. Pei, F.; An, T.; Zang, J.; Zhao, X.; Fang, X.; Zheng, M.; Dong, Q.; Zheng, N. From hollow carbon spheres to N-doped hollow porous carbon bowls: Rational design of hollow carbon host for Li-S batteries. *Adv. Energy Mater.* **2016**, *6*, 1502539. [[CrossRef](#)]
17. Evers, C.H.; Luiken, J.A.; Bolhuis, P.G.; Kegel, W.K. Self-assembly of microcapsules via colloidal bond hybridization and anisotropy. *Nature* **2016**, *534*, 364–368. [[CrossRef](#)]
18. Hu, X.; Hu, J.; Tian, J.; Ge, Z.; Zhang, G.; Luo, K.; Liu, S. Polyprodrug amphiphiles: Hierarchical assemblies for shape-regulated cellular internalization, trafficking, and drug delivery. *J. Am. Chem. Soc.* **2013**, *135*, 17617–17629. [[CrossRef](#)]

19. Zhang, W.; Wang, C.; Chen, K.; Yin, Y. Raspberry-shaped thermochromic energy storage nanocapsule with tunable sunlight absorption based on color change for temperature regulation. *Small* **2019**, *15*, 1903750. [CrossRef]
20. He, J.; Liu, Y.; Hood, T.C.; Zhang, P.; Gong, J.; Nie, Z. Asymmetric organic/metal (oxide) hybrid nanoparticles: Synthesis and applications. *Nanoscale* **2013**, *5*, 5151–5166. [CrossRef]
21. Klein, J. Probing the interactions of proteins and nanoparticles. *Proc. Natl. Acad. Sci. USA* **2007**, *104*, 2029–2030. [CrossRef]
22. Gholami, R.M.; Borghei, S.; Mousavi, S. Heavy metals recovery from spent catalyst using *Acidithiobacillus ferrooxidans* and *Acidithiobacillus thiooxidans*. In Proceedings of the 2010 International Conference on Chemistry and Chemical Engineering, Kyoto, Japan, 1–3 August 2010; pp. 331–335.
23. Mousavi, S.M.; Hashemi, S.A.; Bahrani, S.; Sadrmousavi-Dizaj, A.; Arjmand, O.; Omidifar, N.; Lai, C.W.; Chiang, W.-H.; Gholami, A. Bioinorganic Synthesis of Sodium Polytungstate/Polyoxometalate in Microbial Kombucha Media for Precise Detection of Doxorubicin. *Bioinorg. Chem. Appl.* **2022**, *2022*, 2265108. [CrossRef] [PubMed]
24. Jia, L.; Li, X.; Liu, H.; Xia, J.; Shi, X.; Shen, M. Ultrasound-enhanced precision tumor theranostics using cell membrane-coated and pH-responsive nanoclusters assembled from ultrasmall iron oxide nanoparticles. *Nano Today* **2021**, *36*, 101022. [CrossRef]
25. Feliciano, C.P.; Tsuboi, K.; Suzuki, K.; Kimura, H.; Nagasaki, Y. Long-term bioavailability of redox nanoparticles effectively reduces organ dysfunctions and death in whole-body irradiated mice. *Biomaterials* **2017**, *129*, 68–82. [CrossRef] [PubMed]
26. Moghimi, S.M.; Szabeni, J. Stealth liposomes and long circulating nanoparticles: Critical issues in pharmacokinetics, opsonization and protein-binding properties. *Prog. Lipid Res.* **2003**, *42*, 463–478. [CrossRef]
27. Mousavi, S.M.; Hashemi, S.A.; Bahrani, S.; Yousefi, K.; Behbudi, G.; Babapoor, A.; Omidifar, N.; Lai, C.W.; Gholami, A.; Chiang, W.-H. Recent advancements in polythiophene-based materials and their biomedical, geno sensor and DNA detection. *Int. J. Mol. Sci.* **2021**, *22*, 6850. [CrossRef]
28. Hashemi, M.; Shojaosadati, S.A.; Razavi, S.H.; Mousavi, S.M. Evaluation of Ca-independent α -Amylase Production by *Bacillus* sp. KR-8104 in Submerged and Solid State Fermentation Systems. Available online: <https://www.sid.ir/paper/139204/en> (accessed on 9 July 2011).
29. Xu, X.; Li, T.; Jin, K. Bioinspired and Biomimetic Nanomedicines for Targeted Cancer Therapy. *Pharmaceutics* **2022**, *14*, 1109. [CrossRef]
30. Hashemi, S.A.; Bahrani, S.; Mousavi, S.M.; Mojoudi, F.; Omidifar, N.; Lankarani, K.B.; Arjmand, M.; Ramakrishna, S. Development of sulfurized Polythiophene-Silver Iodide-Diethylthiocarbamate nanoflakes toward Record-High and selective absorption and detection of mercury derivatives in aquatic substrates. *Chem. Eng. J.* **2022**, *440*, 135896. [CrossRef]
31. Mousavi, S.M.; Hashemi, S.A.; Esmaili, H.; Amani, A.M.; Mojoudi, F. Synthesis of Fe₃O₄ nanoparticles modified by oak shell for treatment of wastewater containing Ni (II). *Acta Chim. Slov.* **2018**, *65*, 750–756. [CrossRef]
32. Hashemi, S.A.; Bahrani, S.; Mousavi, S.M.; Omidifar, N.; Arjmand, M.; Behbahan, N.G.G.; Ramakrishna, S.; Lankarani, K.B.; Moghadami, M.; Firoozsani, M. Ultrasensitive Biomolecule-Less Nanosensor Based on β -Cyclodextrin/Quinoline Decorated Graphene Oxide toward Prompt and Differentiable Detection of Corona and Influenza Viruses. *Adv. Mater. Technol.* **2021**, *6*, 2100341. [CrossRef]
33. Mousavi, S.M.; Hashemi, S.A.; Ghahramani, Y.; Azhdari, R.; Yousefi, K.; Gholami, A.; Fallahi Nezhad, F.; Vijayakameswara Rao, N.; Omidifar, N.; Chiang, W.-H. Antiproliferative and Apoptotic Effects of Graphene Oxide@AlF₃ MOF Based Saponin Natural Product on OSCC Line. *Pharmaceutics* **2022**, *15*, 1137. [CrossRef]
34. Hashemi, S.A.; Bahrani, S.; Mousavi, S.M.; Omidifar, N.; Arjmand, M.; Lankarani, K.B.; Ramakrishna, S. Simultaneous electrochemical detection of Cd and Pb in aquatic samples via coupled graphene with brominated white polyaniline flakes. *Eur. Polym. J.* **2022**, *162*, 110926. [CrossRef]
35. Mousavi, S.M.; Hashemi, S.A.; Ghasemi, Y.; Amani, A.M.; Babapoor, A.; Arjmand, O. Applications of graphene oxide in case of nanomedicines and nanocarriers for biomolecules: Review study. *Drug Metab. Rev.* **2019**, *51*, 12–41. [CrossRef] [PubMed]
36. Li, X.; Zhou, L.; Wei, Y.; El-Toni, A.M.; Zhang, F.; Zhao, D. Anisotropic growth-induced synthesis of dual-compartment Janus mesoporous silica nanoparticles for bimodal triggered drugs delivery. *J. Am. Chem. Soc.* **2014**, *136*, 15086–15092. [CrossRef] [PubMed]
37. Mousavi, S.M.; Hashemi, S.A.; Gholami, A.; Kalashgrani, M.Y.; Vijayakameswara Rao, N.; Omidifar, N.; Hsiao, W.W.-W.; Lai, C.W.; Chiang, W.-H. Plasma-Enabled Smart Nanoexosome Platform as Emerging Immunopathogenesis for Clinical Viral Infection. *Pharmaceutics* **2022**, *14*, 1054. [CrossRef]
38. Mousavi, S.M.; Hashemi, S.A.; Gholami, A.; Omidifar, N.; Zarei, M.; Bahrani, S.; Yousefi, K.; Chiang, W.-H.; Babapoor, A. Bioinorganic synthesis of polyrhodanine stabilized Fe₃O₄/Graphene oxide in microbial supernatant media for anticancer and antibacterial applications. *Bioinorg. Chem. Appl.* **2021**, *2021*, 9972664. [CrossRef]
39. Deng, R.; Liang, F.; Qu, X.; Wang, Q.; Zhu, J.; Yang, Z. Diblock copolymer based Janus nanoparticles. *Macromolecules* **2015**, *48*, 750–755. [CrossRef]
40. Cheng, L.; Hou, G.; Miao, J.; Chen, D.; Jiang, M.; Zhu, L. Efficient synthesis of unimolecular polymeric Janus nanoparticles and their unique self-assembly behavior in a common solvent. *Macromolecules* **2008**, *41*, 8159–8166. [CrossRef]
41. Wang, X.; Feng, X.; Ma, G.; Yao, L.; Ge, M. Amphiphilic Janus Particles Generated via a Combination of Diffusion-Induced Phase Separation and Magnetically Driven Dewetting and Their Synergistic Self-Assembly. *Adv. Mater.* **2016**, *28*, 3131–3137. [CrossRef]

42. Hashemi, S.A.; Bahrani, S.; Mousavi, S.M.; Omidifar, N.; Behbahan, N.G.G.; Arjmand, M.; Ramakrishna, S.; Lankarani, K.B.; Moghadami, M.; Shokripour, M. Ultra-precise label-free nanosensor based on integrated graphene with Au nanostars toward direct detection of IgG antibodies of SARS-CoV-2 in blood. *J. Electroanal. Chem.* **2021**, *894*, 115341. [[CrossRef](#)]
43. Mousavi, S.M.; Hashemi, S.A.; Iman Moezzi, S.M.; Ravan, N.; Gholami, A.; Lai, C.W.; Chiang, W.-H.; Omidifar, N.; Yousefi, K.; Behbudi, G. Recent advances in enzymes for the bioremediation of pollutants. *Biochem. Res. Int.* **2021**, *2021*, 5599204. [[CrossRef](#)]
44. Oguzturk, H.E.; Sozen, Y.; Akyol, C.; Ozkendir Inanc, D.; Yildiz, U.H.; Sahin, H. Toward single-layer Janus crystals: Off-balance materials from synthesis to nanotechnology applications. *J. Appl. Phys.* **2021**, *129*, 160902. [[CrossRef](#)]
45. Zhang, Y.; Huang, K.; Lin, J.; Huang, P. Janus nanoparticles in cancer diagnosis, therapy and theranostics. *Biomater. Sci.* **2019**, *7*, 1262–1275. [[CrossRef](#)] [[PubMed](#)]
46. Mousavi, S.M.; Hashemi, S.A.; Kalashgrani, M.Y.; Gholami, A.; Omidifar, N.; Babapoor, A.; Vijayakameswara Rao, N.; Chiang, W.-H. Recent Advances in Plasma-Engineered Polymers for Biomarker-Based Viral Detection and Highly Multiplexed Analysis. *Biosensors* **2022**, *12*, 286. [[CrossRef](#)] [[PubMed](#)]
47. Zhang, X.; Fu, Q.; Duan, H.; Song, J.; Yang, H. Janus nanoparticles: From fabrication to (bio) applications. *ACS Nano* **2021**, *15*, 6147–6191. [[CrossRef](#)]
48. Hashemi, S.A.; Karimipourfard, M.; Mousavi, S.M.; Sina, S.; Bahrani, S.; Omidifar, N.; Ramakrishna, S.; Arjmand, M. Transparent Sodium Polytungstate Polyoxometalate Aquatic Shields Toward Effective X-ray Radiation Protection: Alternative to Lead Glasses. *Mater. Today Commun.* **2022**, *31*, 103822. [[CrossRef](#)]
49. Mousavi, S.M.; Hashemi, S.A.; Kalashgrani, M.Y.; Omidifar, N.; Bahrani, S.; Vijayakameswara Rao, N.; Babapoor, A.; Gholami, A.; Chiang, W.-H. Bioactive Graphene Quantum Dots Based Polymer Composite for Biomedical Applications. *Polymers* **2022**, *14*, 617. [[CrossRef](#)] [[PubMed](#)]
50. Tran, L.-T.-C.; Lesieur, S.; Faivre, V. Janus nanoparticles: Materials, preparation and recent advances in drug delivery. *Expert Opin. Drug Deliv.* **2014**, *11*, 1061–1074. [[CrossRef](#)]
51. Luo, M.; Feng, Y.; Wang, T.; Guan, J. Micro-/nanorobots at work in active drug delivery. *Adv. Funct. Mater.* **2018**, *28*, 1706100. [[CrossRef](#)]
52. Hashemi, S.A.; Mousavi, S.M.; Arjmand, M.; Yan, N.; Sundararaj, U. Electrified single-walled carbon nanotube/epoxy nanocomposite via vacuum shock technique: Effect of alignment on electrical conductivity and electromagnetic interference shielding. *Polym. Compos.* **2018**, *39*, E1139–E1148. [[CrossRef](#)]
53. Mousavi, S.M.; Hashemi, S.A.; Mazraedoost, S.; Yousefi, K.; Gholami, A.; Behbudi, G.; Ramakrishna, S.; Omidifar, N.; Alizadeh, A.; Chiang, W.-H. Multifunctional gold nanorod for therapeutic applications and pharmaceutical delivery considering cellular metabolic responses, oxidative stress and cellular longevity. *Nanomaterials* **2021**, *11*, 1868. [[CrossRef](#)]
54. Gillies, E.R.; Frechet, J.M. Dendrimers and dendritic polymers in drug delivery. *Drug Discov. Today* **2005**, *10*, 35–43. [[CrossRef](#)] [[PubMed](#)]
55. Hashemi, S.A.; Mousavi, S.M.; Bahrani, S.; Gholami, A.; Chiang, W.-H.; Yousefi, K.; Omidifar, N.; Rao, N.V.; Ramakrishna, S.; Babapoor, A. Bio-enhanced polyrhodanine/graphene Oxide/Fe₃O₄ nanocomposite with kombucha solvent supernatant as ultra-sensitive biosensor for detection of doxorubicin hydrochloride in biological fluids. *Mater. Chem. Phys.* **2022**, *279*, 125743. [[CrossRef](#)]
56. Mousavi, S.M.; Hashemi, S.A.; Parvin, N.; Gholami, A.; Ramakrishna, S.; Omidifar, N.; Moghadami, M.; Chiang, W.-H.; Mazraedoost, S. Recent biotechnological approaches for treatment of novel COVID-19: From bench to clinical trial. *Drug Metab. Rev.* **2021**, *53*, 141–170. [[CrossRef](#)] [[PubMed](#)]
57. Acton, A.L.; Fante, C.; Flatley, B.; Burattini, S.; Hamley, I.W.; Wang, Z.; Greco, F.; Hayes, W. Janus PEG-based dendrimers for use in combination therapy: Controlled multi-drug loading and sequential release. *Biomacromolecules* **2013**, *14*, 564–574. [[CrossRef](#)] [[PubMed](#)]
58. Mousavi, S.M.; Hashemi, S.A.; Ramakrishna, S.; Esmaeili, H.; Bahrani, S.; Koosha, M.; Babapoor, A. Green synthesis of supermagnetic Fe₃O₄-MgO nanoparticles via Nutmeg essential oil toward superior anti-bacterial and anti-fungal performance. *J. Drug Deliv. Sci. Technol.* **2019**, *54*, 101352. [[CrossRef](#)]
59. Huang, D.; Wu, D. Biodegradable dendrimers for drug delivery. *Mater. Sci. Eng. C* **2018**, *90*, 713–727. [[CrossRef](#)]
60. Sanchez, L.; Yi, Y.; Yu, Y. Effect of partial PEGylation on particle uptake by macrophages. *Nanoscale* **2017**, *9*, 288–297. [[CrossRef](#)]
61. Hashemi, S.A.; Mousavi, S.M.; Bahrani, S.; Omidifar, N.; Arjmand, M.; Ramakrishna, S.; Hagfeldt, A.; Lankarani, K.B.; Chiang, W.-H. Decorated graphene oxide flakes with integrated complex of 8-hydroxyquinoline/NiO toward accurate detection of glucose at physiological conditions. *J. Electroanal. Chem.* **2021**, *893*, 115303. [[CrossRef](#)]
62. Mousavi, S.M.; Hashemi, S.A.; Yari Kalashgrani, M.; Omidifar, N.; Lai, C.W.; Vijayakameswara Rao, N.; Gholami, A.; Chiang, W.-H. The Pivotal Role of Quantum Dots-Based Biomarkers Integrated with Ultra-Sensitive Probes for Multiplex Detection of Human Viral Infections. *Pharmaceuticals* **2022**, *15*, 880. [[CrossRef](#)]
63. Xie, H.; She, Z.-G.; Wang, S.; Sharma, G.; Smith, J.W. One-step fabrication of polymeric Janus nanoparticles for drug delivery. *Langmuir* **2012**, *28*, 4459–4463. [[CrossRef](#)]
64. Mousavi, S.M.; Hashemi, S.A.; Zarei, M.; Amani, A.M.; Babapoor, A. Nanosensors for chemical and biological and medical applications. *Med. Chem.* **2018**, *8*, 205–217. [[CrossRef](#)]
65. Schick, I.; Lorenz, S.; Gehrig, D.; Tenzer, S.; Storck, W.; Fischer, K.; Strand, D.; Laquai, F.; Tremel, W. Inorganic Janus particles for biomedical applications. *Beilstein J. Nanotechnol.* **2014**, *5*, 2346–2362. [[CrossRef](#)] [[PubMed](#)]

66. Feng, Z.-Q.; Yan, K.; Li, J.; Xu, X.; Yuan, T.; Wang, T.; Zheng, J. Magnetic Janus particles as a multifunctional drug delivery system for paclitaxel in efficient cancer treatment. *Mater. Sci. Eng. C* **2019**, *104*, 110001. [[CrossRef](#)] [[PubMed](#)]
67. Reguera, J.; de Aberasturi, D.J.; Henriksen-Lacey, M.; Langer, J.; Espinosa, A.; Szczupak, B.; Wilhelm, C.; Liz-Marzán, L.M. Janus plasmonic–magnetic gold–iron oxide nanoparticles as contrast agents for multimodal imaging. *Nanoscale* **2017**, *9*, 9467–9480. [[CrossRef](#)] [[PubMed](#)]
68. Hashemi, S.A.; Mousavi, S.M.; Bahrani, S.; Ramakrishna, S. Integrated polyaniline with graphene oxide-iron tungsten nitride nanoflakes as ultrasensitive electrochemical sensor for precise detection of 4-nitrophenol within aquatic media. *J. Electroanal. Chem.* **2020**, *873*, 114406. [[CrossRef](#)]
69. Mousavi, S.M.; Hashemi, S.A.; Zarei, M.; Bahrani, S.; Savardashtaki, A.; Esmaili, H.; Lai, C.W.; Mazraedoost, S.; Abassi, M.; Ramavandi, B. Data on cytotoxic and antibacterial activity of synthesized Fe_3O_4 nanoparticles using *Malva sylvestris*. *Data Brief* **2020**, *28*, 104929. [[CrossRef](#)] [[PubMed](#)]
70. Mousavi, S.M.; Hashemi, S.A.; Zarei, M.; Gholami, A.; Lai, C.W.; Chiang, W.H.; Omidifar, N.; Bahrani, S.; Mazraedoost, S. Recent progress in chemical composition, production, and pharmaceutical effects of kombucha beverage: A complementary and alternative medicine. *Evid.-Based Complement. Altern. Med.* **2020**, *2020*, 4397543. [[CrossRef](#)] [[PubMed](#)]
71. Lee, K.; Yu, Y. Janus nanoparticles for T cell activation: Clustering ligands to enhance stimulation. *J. Mater. Chem. B* **2017**, *5*, 4410–4415. [[CrossRef](#)]
72. Wang, Z.; Shao, D.; Chang, Z.; Lu, M.; Wang, Y.; Yue, J.; Yang, D.; Li, M.; Xu, Q.; Dong, W.-f. Janus gold nanoplatform for synergetic chemoradiotherapy and computed tomography imaging of hepatocellular carcinoma. *ACS Nano* **2017**, *11*, 12732–12741. [[CrossRef](#)]
73. Mousavi, S.M.; Low, F.W.; Hashemi, S.A.; Samsudin, N.A.; Shakeri, M.; Yusoff, Y.; Rahsepar, M.; Lai, C.W.; Babapoor, A.; Soroshnia, S. Development of hydrophobic reduced graphene oxide as a new efficient approach for photochemotherapy. *RSC Adv.* **2020**, *10*, 12851–12863. [[CrossRef](#)]
74. Efremova, M.V.; Naumenko, V.A.; Spasova, M.; Garanina, A.S.; Abakumov, M.A.; Blokhina, A.D.; Melnikov, P.A.; Prelovskaya, A.O.; Heidelmann, M.; Li, Z.-A. Magnetite-Gold nanohybrids as ideal all-in-one platforms for theranostics. *Sci. Rep.* **2018**, *8*, 11295. [[CrossRef](#)] [[PubMed](#)]
75. Mousavi, S.M.; Soroshnia, S.; Hashemi, S.A.; Babapoor, A.; Ghasemi, Y.; Savardashtaki, A.; Amani, A.M. Graphene nano-ribbon based high potential and efficiency for DNA, cancer therapy and drug delivery applications. *Drug Metab. Rev.* **2019**, *51*, 91–104. [[CrossRef](#)] [[PubMed](#)]
76. Wang, F.; Pauletti, G.M.; Wang, J.; Zhang, J.; Ewing, R.C.; Wang, Y.; Shi, D. Dual surface-functionalized janus nanocomposites of polystyrene/ $\text{Fe}_3\text{O}_4@ \text{SiO}_2$ for simultaneous tumor cell targeting and stimulus-induced drug release. *Adv. Mater.* **2013**, *25*, 3485–3489. [[CrossRef](#)] [[PubMed](#)]
77. Hashemi, S.A.; Mousavi, S.M.; Bahrani, S.; Ramakrishna, S.; Hashemi, S.H. Picomolar-level detection of mercury within non-biological/biological aqueous media using ultra-sensitive polyaniline- Fe_3O_4 -silver diethyldithiocarbamate nanostructure. *Anal. Bioanal. Chem.* **2020**, *412*, 5353–5365. [[CrossRef](#)]
78. Mousavi, S.M.; Yousefi, K.; Hashemi, S.A.; Afza, M.; Bahrani, S.; Gholami, A.; Ghahramani, Y.; Alizadeh, A.; Chiang, W.-H. Renewable carbon nanomaterials: Novel resources for dental tissue engineering. *Nanomaterials* **2021**, *11*, 2800. [[CrossRef](#)]
79. Mousavi, S.M.; Zarei, M.; Hashemi, S.A.; Babapoor, A.; Amani, A.M. A conceptual review of rhodanine: Current applications of antiviral drugs, anticancer and antimicrobial activities. *Artif. Cells Nanomed. Biotechnol.* **2019**, *47*, 1132–1148. [[CrossRef](#)]
80. Park, J.H.; Dumani, D.S.; Arsiwala, A.; Emelianov, S.; Kane, R.S. Tunable aggregation of gold-silica janus nanoparticles to enable contrast-enhanced multiwavelength photoacoustic imaging in vivo. *Nanoscale* **2018**, *10*, 15365–15370. [[CrossRef](#)]
81. Fang, L.; Wang, W.; Liu, Y.; Xie, Z.; Chen, L. Janus nanostructures formed by mesoporous silica coating Au nanorods for near-infrared chemo–photothermal therapy. *J. Mater. Chem. B* **2017**, *5*, 8833–8838. [[CrossRef](#)]
82. Zhang, Q.; Zhang, L.; Li, S.; Chen, X.; Zhang, M.; Wang, T.; Li, L.; Wang, C. Designed synthesis of $\text{Au}/\text{Fe}_3\text{O}_4@ \text{C}$ Janus nanoparticles for dual-modal imaging and actively targeted chemo-photothermal synergistic therapy of cancer cells. *Chem.–A Eur. J.* **2017**, *23*, 17242–17248. [[CrossRef](#)]
83. Cao, H.; Yang, Y.; Chen, X.; Shao, Z. Intelligent Janus nanoparticles for intracellular real-time monitoring of dual drug release. *Nanoscale* **2016**, *8*, 6754–6760. [[CrossRef](#)]
84. Wang, Z.; Chang, Z.; Lu, M.; Shao, D.; Yue, J.; Yang, D.; Zheng, X.; Li, M.; He, K.; Zhang, M. Shape-controlled magnetic mesoporous silica nanoparticles for magnetically-mediated suicide gene therapy of hepatocellular carcinoma. *Biomaterials* **2018**, *154*, 147–157. [[CrossRef](#)] [[PubMed](#)]
85. Shao, D.; Li, J.; Zheng, X.; Pan, Y.; Wang, Z.; Zhang, M.; Chen, Q.-X.; Dong, W.-F.; Chen, L. Janus “nano-bullets” for magnetic targeting liver cancer chemotherapy. *Biomaterials* **2016**, *100*, 118–133. [[CrossRef](#)]
86. Shao, D.; Zhang, X.; Liu, W.; Zhang, F.; Zheng, X.; Qiao, P.; Li, J.; Dong, W.-f.; Chen, L. Janus silver-mesoporous silica nanocarriers for SERS traceable and pH-sensitive drug delivery in cancer therapy. *ACS Appl. Mater. Interfaces* **2016**, *8*, 4303–4308. [[CrossRef](#)] [[PubMed](#)]
87. Hu, S.-H.; Chen, S.-Y.; Gao, X. Multifunctional nanocapsules for simultaneous encapsulation of hydrophilic and hydrophobic compounds and on-demand release. *ACS Nano* **2012**, *6*, 2558–2565. [[CrossRef](#)] [[PubMed](#)]
88. Wang, Y.; Ji, X.; Pang, P.; Shi, Y.; Dai, J.; Xu, J.; Wu, J.; Kirk, T.B.; Xue, W. Synthesis of Janus Au nanorods/polydivinylbenzene hybrid nanoparticles for chemo-photothermal therapy. *J. Mater. Chem. B* **2018**, *6*, 2481–2488. [[CrossRef](#)]

89. Wang, H.; Li, S.; Zhang, L.; Chen, X.; Wang, T.; Zhang, M.; Li, L.; Wang, C. Tunable fabrication of folic acid-Au@ poly (acrylic acid)/mesoporous calcium phosphate Janus nanoparticles for CT imaging and active-targeted chemotherapy of cancer cells. *Nanoscale* **2017**, *9*, 14322–14326. [[CrossRef](#)]
90. Zhao, T.; Elzatahry, A.; Li, X.; Zhao, D. Single-micelle-directed synthesis of mesoporous materials. *Nat. Rev. Mater.* **2019**, *4*, 775–791. [[CrossRef](#)]
91. Hashemi, S.A.; Mousavi, S.M.; Faghihi, R.; Arjmand, M.; Rahsepar, M.; Bahrani, S.; Ramakrishna, S.; Lai, C.W. Superior X-ray radiation shielding effectiveness of biocompatible polyaniline reinforced with hybrid graphene oxide-iron tungsten nitride flakes. *Polymers* **2020**, *12*, 1407. [[CrossRef](#)]
92. Wan, Y.; Zhao, D. On the controllable soft-templating approach to mesoporous silicates. *Chem. Rev.* **2007**, *107*, 2821–2860. [[CrossRef](#)]
93. Li, C.; Iqbal, M.; Lin, J.; Luo, X.; Jiang, B.; Malgras, V.; Wu, K.C.-W.; Kim, J.; Yamauchi, Y. Electrochemical deposition: An advanced approach for templated synthesis of nanoporous metal architectures. *Acc. Chem. Res.* **2018**, *51*, 1764–1773. [[CrossRef](#)]
94. Mousavi, S.M.; Zarei, M.; Hashemi, S.A.; Ramakrishna, S.; Chiang, W.-H.; Lai, C.W.; Gholami, A. Gold nanostars-diagnosis, bioimaging and biomedical applications. *Drug Metab. Rev.* **2020**, *52*, 299–318. [[CrossRef](#)] [[PubMed](#)]
95. Zhao, T.; Chen, L.; Lin, R.; Zhang, P.; Lan, K.; Zhang, W.; Li, X.; Zhao, D. Interfacial assembly directed unique mesoporous architectures: From symmetric to asymmetric. *Acc. Mater. Res.* **2020**, *1*, 100–114. [[CrossRef](#)]
96. Cheng, Y.; Zhang, Y.; Deng, W.; Hu, J. Antibacterial and anticancer activities of asymmetric lollipop-like mesoporous silica nanoparticles loaded with curcumin and gentamicin sulfate. *Colloids Surf. B Biointerfaces* **2020**, *186*, 110744. [[CrossRef](#)] [[PubMed](#)]
97. Hashemi, S.A.; Mousavi, S.M.; Naderi, H.R.; Bahrani, S.; Arjmand, M.; Hagfeldt, A.; Chiang, W.-H.; Ramakrishna, S. Reinforced polypyrrole with 2D graphene flakes decorated with interconnected nickel-tungsten metal oxide complex toward superiorly stable supercapacitor. *Chem. Eng. J.* **2021**, *418*, 129396. [[CrossRef](#)]
98. Mousavi, S.M.; Zarei, M.; Hashemi, S.A.; Ramakrishna, S.; Chiang, W.-H.; Lai, C.W.; Gholami, A.; Omidifar, N.; Shokripour, M. Asymmetric membranes: A potential scaffold for wound healing applications. *Symmetry* **2020**, *12*, 1100. [[CrossRef](#)]
99. Abbaraju, P.L.; Jambhrunkar, M.; Yang, Y.; Liu, Y.; Lu, Y.; Yu, C. Asymmetric mesoporous silica nanoparticles as potent and safe immunoadjuvants provoke high immune responses. *Chem. Commun.* **2018**, *54*, 2020–2023. [[CrossRef](#)]
100. Hashemi, S.A.; Mousavi, S.M.; Ramakrishna, S. Effective removal of mercury, arsenic and lead from aqueous media using Polyaniline-Fe₃O₄-silver diethyldithiocarbamate nanostructures. *J. Clean. Prod.* **2019**, *239*, 118023. [[CrossRef](#)]
101. Li, X.; Zhou, L.; Wei, Y.; El-Toni, A.M.; Zhang, F.; Zhao, D. Anisotropic encapsulation-induced synthesis of asymmetric single-hole mesoporous nanocages. *J. Am. Chem. Soc.* **2015**, *137*, 5903–5906. [[CrossRef](#)]
102. Fallahinezhad, F.; Afsa, M.; Ghahramani, Y. Graphene Quantum Dots and their applications in regenerative medicine: A mini-review. *Adv. Appl. NanoBio-Technol.* **2021**, *4*, 53–59.
103. Nematollahzadeh, A.; Babapoor, A.; Mousavi, S.M.; Nuri, A. Nitrobenzene adsorption from aqueous solution onto polythiophene-modified magnetite nanoparticles. *Mater. Chem. Phys.* **2021**, *262*, 124266. [[CrossRef](#)]
104. Wu, H.; Shen, L.; Zhu, Z.; Luo, X.; Zhai, Y.; Hua, X.; Zhao, S.; Cen, L.; Zhang, Z. A cell-free therapy for articular cartilage repair based on synergistic delivery of SDF-1 & KGN with HA injectable scaffold. *Chem. Eng. J.* **2020**, *393*, 124649.
105. Hassan, N.; Shahat, A.; El-Didamony, A.; El-Desouky, M.; El-Bindary, A. Synthesis and characterization of ZnO nanoparticles via zeolitic imidazolate framework-8 and its application for removal of dyes. *J. Mol. Struct.* **2020**, *1210*, 128029. [[CrossRef](#)]
106. Ayyanaar, S.; Kesavan, M.P.; Balachandran, C.; Rasala, S.; Rameshkumar, P.; Aoki, S.; Rajesh, J.; Webster, T.J.; Rajagopal, G. Iron oxide nanoparticle core-shell magnetic microspheres: Applications toward targeted drug delivery. *Nanomed. Nanotechnol. Biol. Med.* **2020**, *24*, 102134. [[CrossRef](#)] [[PubMed](#)]
107. Zhang, H.; Xu, H.; Wu, M.; Zhong, Y.; Wang, D.; Jiao, Z. A soft-hard template approach towards hollow mesoporous silica nanoparticles with rough surfaces for controlled drug delivery and protein adsorption. *J. Mater. Chem. B* **2015**, *3*, 6480–6489. [[CrossRef](#)]
108. Hosseini, H.; Mousavi, S.M. Density functional theory simulation for Cr (VI) removal from wastewater using bacterial cellulose/polyaniline. *Int. J. Biol. Macromol.* **2020**, *165*, 883–901. [[CrossRef](#)]
109. Wang, Z.; Zhang, F.; Shao, D.; Chang, Z.; Wang, L.; Hu, H.; Zheng, X.; Li, X.; Chen, F.; Tu, Z. Janus nanobullets combine photodynamic therapy and magnetic hyperthermia to potentiate synergetic anti-metastatic immunotherapy. *Adv. Sci.* **2019**, *6*, 1901690. [[CrossRef](#)]
110. Chang, Z.-m.; Wang, Z.; Lu, M.-m.; Shao, D.; Yue, J.; Yang, D.; Li, M.-q.; Dong, W.-f. Janus silver mesoporous silica nanobullets with synergistic antibacterial functions. *Colloids Surf. B Biointerfaces* **2017**, *157*, 199–206. [[CrossRef](#)]
111. Wang, Z.; Chang, Z.; Lu, M.; Shao, D.; Yue, J.; Yang, D.; Li, M.; Dong, W.-f. Janus silver/silica nanoplatfoms for light-activated liver cancer chemo/photothermal therapy. *ACS Appl. Mater. Interfaces* **2017**, *9*, 30306–30317. [[CrossRef](#)]
112. Wang, Z.; Wang, Y.; Lu, M.; Li, L.; Zhang, Y.; Zheng, X.; Shao, D.; Li, J.; Dong, W.-f. Janus Au-mesoporous silica nanocarriers for chemo-photothermal treatment of liver cancer cells. *RSC Adv.* **2016**, *6*, 44498–44505. [[CrossRef](#)]
113. Zhang, L.; Chen, Y.; Li, Z.; Li, L.; Saint-Cricq, P.; Li, C.; Lin, J.; Wang, C.; Su, Z.; Zink, J.I. Tailored synthesis of octopus-type janus nanoparticles for synergistic actively-targeted and chemo-photothermal therapy. *Angew. Chem. Int. Ed.* **2016**, *55*, 2118–2121. [[CrossRef](#)]
114. Xiong, L.; Qiao, S.-Z. A mesoporous organosilica nano-bowl with high DNA loading capacity—a potential gene delivery carrier. *Nanoscale* **2016**, *8*, 17446–17450. [[CrossRef](#)] [[PubMed](#)]

115. Hosseini, H.; Mousavi, S.M. Bacterial cellulose/polyaniline nanocomposite aerogels as novel bioadsorbents for removal of hexavalent chromium: Experimental and simulation study. *J. Clean. Prod.* **2021**, *278*, 123817. [[CrossRef](#)]
116. Hosseini, H.; Mousavi, S.M.; Wurm, F.R.; Goodarzi, V. Display of hidden properties of flexible aerogel based on bacterial cellulose/polyaniline nanocomposites with helping of multiscale modeling. *Eur. Polym. J.* **2021**, *146*, 110251. [[CrossRef](#)]
117. López, V.; Villegas, M.R.; Rodríguez, V.; Villaverde, G.; Lozano, D.; Baeza, A.; Vallet-Regí, M. Janus mesoporous silica nanoparticles for dual targeting of tumor cells and mitochondria. *ACS Appl. Mater. Interfaces* **2017**, *9*, 26697–26706. [[CrossRef](#)]
118. Vallet-Regí, M.; Colilla, M.; Izquierdo-Barba, I.; Manzano, M. Mesoporous silica nanoparticles for drug delivery: Current insights. *Molecules* **2017**, *23*, 47. [[CrossRef](#)]
119. Wan, M.; Wang, Q.; Li, X.; Xu, B.; Fang, D.; Li, T.; Yu, Y.; Fang, L.; Wang, Y.; Wang, M. Systematic research and evaluation models of nanomotors for cancer combined therapy. *Angew. Chem. Int. Ed.* **2020**, *59*, 14458–14465. [[CrossRef](#)]
120. Gao, C.; Wang, Y.; Ye, Z.; Lin, Z.; Ma, X.; He, Q. Biomedical micro-/nanomotors: From overcoming biological barriers to in vivo imaging. *Adv. Mater.* **2021**, *33*, 2000512. [[CrossRef](#)]
121. Llopis-Lorente, A.; García-Fernández, A.; Lucena-Sánchez, E.; Díez, P.; Sancenón, F.; Villalonga, R.; Wilson, D.A.; Martínez-Manez, R. Stimulus-responsive nanomotors based on gated enzyme-powered Janus Au-mesoporous silica nanoparticles for enhanced cargo delivery. *Chem. Commun.* **2019**, *55*, 13164–13167. [[CrossRef](#)]
122. Jafari, A.; Zamankhan, P.; Mousavi, S.M.; Henttinen, K. Multiscale modeling of fluid turbulence and flocculation in fiber suspensions. *J. Appl. Phys.* **2006**, *100*, 034901. [[CrossRef](#)]
123. Kalashgarani, M.Y.; Babapoor, A. Application of nano-antibiotics in the diagnosis and treatment of infectious diseases. *Adv. Appl. NanoBio-Technol.* **2022**, *3*, 22–35.
124. Wang, Z.; Chang, Z.-m.; Shao, D.; Zhang, F.; Chen, F.; Li, L.; Ge, M.-f.; Hu, R.; Zheng, X.; Wang, Y. Janus gold triangle-mesoporous silica nanoplatforms for hypoxia-activated radio-chemo-photothermal therapy of liver cancer. *ACS Appl. Mater. Interfaces* **2019**, *11*, 34755–34765. [[CrossRef](#)] [[PubMed](#)]
125. Kalashgrani, M.Y.; Harzand, F.V.; Javanmardi, N.; Nejad, F.F.; Rahmanian, V. Recent Advances in Multifunctional magnetic nano platform for Biomedical Applications: A mini review. *Adv. Appl. NanoBio-Technol.* **2022**, *3*, 31–37.
126. Malik, P.; Katyal, V.; Malik, V.; Asatkar, A.; Inwati, G.; Mukherjee, T.K. Nanobiosensors: Concepts and variations. *Int. Sch. Res. Not.* **2013**, *2013*, 327435. [[CrossRef](#)]
127. Kalashgrani, M.Y.; Javanmardi, N. Multifunctional Gold nanoparticle: As novel agents for cancer treatment. *Adv. Appl. NanoBio-Technol.* **2022**, *in press*.
128. Azimzadeh, M.; Rahaie, M.; Nasirizadeh, N.; Ashtari, K.; Naderi-Manesh, H. An electrochemical nanobiosensor for plasma miRNA-155, based on graphene oxide and gold nanorod, for early detection of breast cancer. *Biosens. Bioelectron.* **2016**, *77*, 99–106. [[CrossRef](#)]
129. Ding, L.; Bond, A.M.; Zhai, J.; Zhang, J. Utilization of nanoparticle labels for signal amplification in ultrasensitive electrochemical affinity biosensors: A review. *Anal. Chim. Acta* **2013**, *797*, 1–12. [[CrossRef](#)] [[PubMed](#)]
130. Kalashgrani, M.Y.; Nejad, F.F.; Rahmanian, V. Carbon Quantum Dots Platforms: As nano therapeutic for Biomedical Applications. *Adv. Appl. NanoBio-Technol.* **2022**, *3*, 38–42.
131. Mousavi, M.; Hashemi, A.; Arjmand, O.; Amani, A.M.; Babapoor, A.; Fateh, M.A.; Fateh, H.; Mojoudi, F.; Esmaeili, H.; Jahandideh, S. Erythrosine adsorption from aqueous solution via decorated graphene oxide with magnetic iron oxide nano particles: Kinetic and equilibrium studies. *Acta Chim. Slov.* **2018**, *65*, 882–894. [[CrossRef](#)]
132. Vigneshvar, S.; Sudhakumari, C.; Senthilkumaran, B.; Prakash, H. Recent advances in biosensor technology for potential applications—an overview. *Front. Bioeng. Biotechnol.* **2016**, *4*, 11. [[CrossRef](#)]
133. Chalasani, K.B.; Russell-Jones, G.; Yandrapu, S.K.; Diwan, P.V.; Jain, S.K. A novel vitamin B12-nanosphere conjugate carrier system for peroral delivery of insulin. *J. Control. Release* **2007**, *117*, 421–429. [[CrossRef](#)]
134. Mousavi, S.; Arjmand, O.; Hashemi, S.; Banaei, N. Modification of the epoxy resin mechanical and thermal properties with silicon acrylate and montmorillonite nanoparticles. *Polym. Renew. Resour.* **2016**, *7*, 101–113. [[CrossRef](#)]
135. Mousavi, S.; Arjmand, O.; Talaghat, M.; Azizi, M.; Shooli, H. Modifying the properties of polypropylene-wood composite by natural polymers and eggshell Nano-particles. *Polym. Renew. Resour.* **2015**, *6*, 157–173. [[CrossRef](#)]
136. Mousavi, S.; Esmaeili, H.; Arjmand, O.; Karimi, S.; Hashemi, S. Biodegradation study of nanocomposites of phenol novolac epoxy/unsaturated polyester resin/egg shell nanoparticles using natural polymers. *J. Mater.* **2015**, *2015*, 131957. [[CrossRef](#)]
137. Dianzani, C.; Zara, G.P.; Maina, G.; Pettazzoni, P.; Pizzimenti, S.; Rossi, F.; Gigliotti, C.L.; Ciamporcerio, E.S.; Daga, M.; Barrera, G. Drug delivery nanoparticles in skin cancers. *BioMed Res. Int.* **2014**, *2014*, 895986. [[CrossRef](#)] [[PubMed](#)]
138. Mousavi, S.; Zarei, M.; Hashemi, S. Polydopamine for biomedical application and drug delivery system. *Med. Chem.* **2018**, *8*, 218–229. [[CrossRef](#)]